

## Study of the Atomic and Electronic Structures of Amorphous Silicon Nitride and Defects in It

S. S. Nekrashevich, A. V. Shaposhnikov, and V. A. Gritsenko

*Institute of Semiconductor Physics, Siberian Branch, Russian Academy of Sciences,  
pr. Akademika Lavrent'eva 13, Novosibirsk, 630090 Russia*

Received July 8, 2010; in final form, June 6, 2011

The structure of amorphous silicon nitride obtained by cooling from a melt has been simulated by Car–Parinello molecular dynamics. Several types of Si–Si defect coordination have been revealed. It has been found that, in addition to normal Si–Si bonds, numerous double Si–Si bonds (Si–Si–Si defects) are present in the amorphous structure.

DOI: 10.1134/S0021364011150082

Flash memory based on silicon nitride is currently being developed. This type of memory devices operates due to the memory effect of silicon nitride, i.e., its capability to capture charge carriers on traps and to keep them for a long time. The nature of traps responsible for the memory effect in silicon nitride is still unclear. One of the hypotheses that explain the nature of traps is a model where a Si–Si bond is considered as a center of capture of electrons and holes. In particular, an increase in the concentration of traps in silicon-enriched Si<sub>3</sub>N<sub>4</sub> [1] is evidence in favor of this model.

A hydrogen-saturated nitrogen vacancy in crystalline β-Si<sub>3</sub>N<sub>4</sub> was proposed as a model for the Si–Si bond in our previous work [2]. The need to introduce a hydrogen atom into the simulated defect was explained by the presence of an unpaired electron in the third silicon atom, which is not involved in the formation of the Si–Si bond. The passivation by the hydrogen atom made it possible to saturate the dangling bond. Subsequent calculations showed that the created defect can be a capture center for both electrons and holes with the localization energies  $\Delta E_e = 1.8$  eV and  $\Delta E_h = 0.9$  eV, respectively. The experimental trap depth is 1.5 eV for both electrons and holes [3]. The difference of the experimental data from theoretical results can be explained by, in particular, the imperfection of the trap model.

In stoichiometric silicon nitride, a silicon atom is coordinated with four nitrogen atoms and a nitrogen atom has three bonds with silicon atoms. Correspondingly, the pure Si–Si bond cannot be analyzed by creating a defect in a crystal cell. The aim of this work is to obtain more reliable information on the structure and Si–Si defect types in amorphous silicon nitride by performing molecular dynamics simulation of its atomic and electronic structures.

The advantage of this method for considering the atomic structure of silicon nitride is that it is not nec-

essary to artificially create defects, which may be absent in real samples. The simulation of the amorphous phase of silicon nitride makes it possible to reveal the statistics and probability of the formation of a certain defect and subsequently to examine the possibility of the localization of carriers on each of the obtained defect types without using any certain model of the Si–Si bond.

It is worth noting that although there are numerous works concerning the nature of traps in silicon nitride, study of defects that are responsible for the memory effect by their simulation in the amorphous phase of silicon nitride has not yet performed. All theoretical investigations were primarily devoted to studying defects that were either artificially created by the cluster method or generated inside the crystal structure. The authors of the overwhelming majority of works devoted to the simulation of amorphous silicon nitride examined the bulk properties of the amorphous structure such as the density of states, radial distribution function, dielectric constant, and X-ray and Raman spectra. No work was devoted to study the types of defects that appear in amorphous nitride. At the same time, the determination of the atomic structure of defects responsible for the capture of a charge is of key importance for revealing the nature of memory traps in silicon nitride. In this work, we attempt for the first time to detect defects based on the Si–Si bond in the amorphous structure of silicon nitride and to ab initio classify them.

The electronic structure of defects was simulated using the Quantum Espresso quantum-mechanical simulation suite [4, 5]. The optimization of the geometry and production of the amorphous atomic structure from the crystal lattice of silicon nitride were performed using the CPMD Car–Parinello molecular dynamics package [6]. The calculations were based on the Hohenberg–Kohn–Sham nonempirical quan-

tum-mechanical method (density functional theory) and Car–Parinello molecular dynamics and involved the exchange correlation functional in the LDA approximation, as well as ultrasoft Vanderbilt pseudopotentials for silicon and nitrogen atoms. The cutoff energy for plane waves was chosen from the calculation of the convergence of the total energy with an accuracy of 0.001 Ry/atom and was 40 Ry.

In this work, the amorphous phase of the silicon nitride was obtained by melting the crystal supercell with subsequent cooling. The first step for obtaining the amorphous structure is the melting of 336-atomic crystal cell of  $\alpha$ -Si<sub>3</sub>N<sub>4</sub>. To accelerate the process of disordering of the crystalline atomic structure upon melting, we chose a temperature of 6000 K. Melting was performed until the complete destruction of the crystalline structure.

We tested several methods for cooling the melt. The simplest and obvious method for cooling the structure obtained after the melting of the crystal is the optimization of the geometry of the high-temperature melt. The optimization of geometry (minimization of forces) was terminated when all three projections of the force acting on each of the atoms reached <0.001 au (Ry/Bohr). In this case, the structure is in the nearest local energy minimum, which corresponds to the instantaneous hardening of the melt. The advantage of this method is the rapidity of obtaining the disordered structure. The main disadvantage is a high concentration of defects that remain after the destruction of the crystal. An analysis of the density of states shows that these defects make a significant contribution to the formation of states in the region of an expected band gap. No pronounced energy gap is observed.

As a result, we decided to perform the melting of the crystal at the minimum possible temperature at which the time necessary for the destruction of the crystalline structure is insufficient for destroying the short-range order. The experimental melting temperature of crystalline silicon nitride is  $\sim$ 2100 K. The threshold temperature obtained in our calculations is much higher ( $\sim$ 4000 K). This is explained by, first, the absence of defects in the structure under consideration, which accelerate melting in real structures, and, second, the short time of the observation of the simulated structure (at a lower temperature, melting would occur but in a longer time interval). Figure 1 shows the radial distribution functions and (b) the total density of states for the structure thus obtained.

In the resulting structure, the concentration of defects is low (a low peak of about 1 at % in the radial distribution function near 1.4 Å, which corresponds to N–N bonds) and a pronounced band gap of 1.5 eV appears. In view of these results, the method described above was chosen as the main method for obtaining the amorphous phase for all subsequent structures.

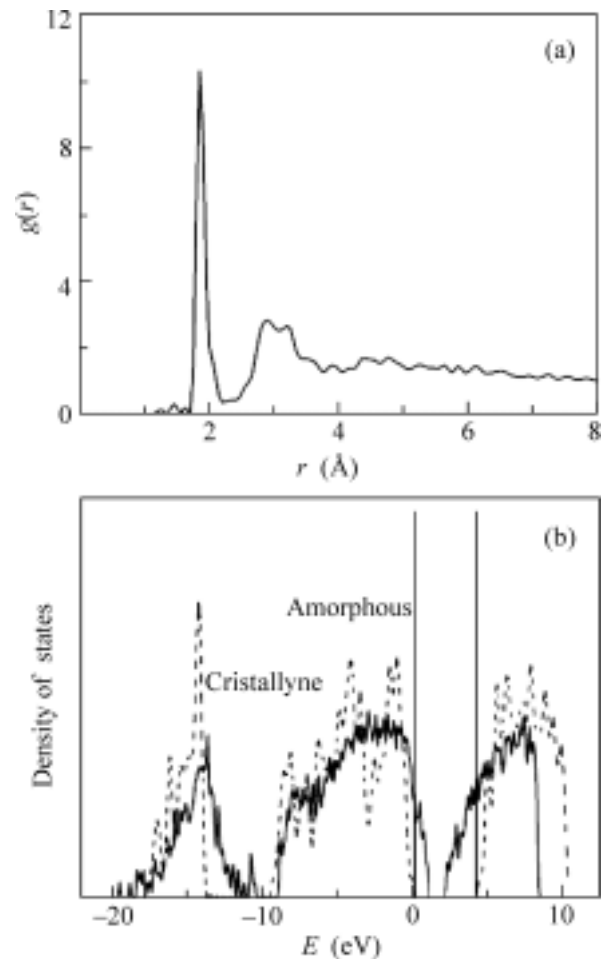


**Fig. 1.** (a) Radial distribution functions and (b) the total density of states for the amorphous structure obtained by optimizing the geometry of the melt (melting at the threshold temperature).

To examine defects associated with silicon excess, we created several amorphous silicon nitride samples of a 336-atomic cell of crystalline  $\alpha$ -Si<sub>3</sub>N<sub>4</sub> with one nitrogen vacancy. The composition of the structure thus obtained is to SiN<sub>1.32</sub> (the stoichiometric composition is SiN<sub>1.33</sub>), which corresponds to enrichment in silicon by about 1 at %. Figure 2 shows the pair distribution functions for the Si–Si and N–N distances.

The broadening of the corresponding peaks indicates that the dispersion of the bond lengths, as well as the interatomic distances in the second and next coordination spheres, increases significantly for all distances after the crystalline–amorphous transition. In addition to an increase in the dispersion of the bond lengths and interatomic distances, their average value increases (the peaks in the Si–N and Si–Si pair distribution functions are shifted towards larger distances). This corresponds to the experimentally observed decrease in the density of the crystalline atomic structure upon its disordering.

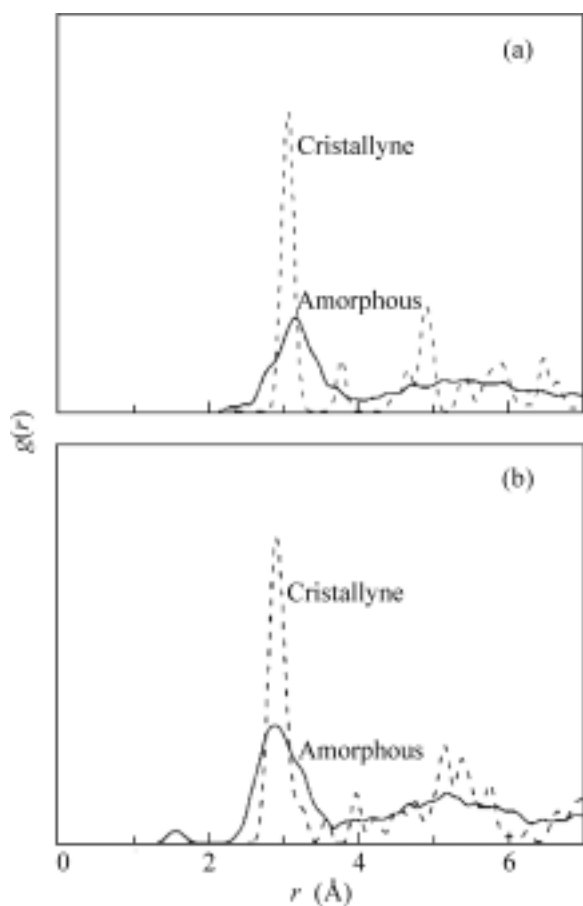


**Fig. 2.** Radial distribution functions and pair distribution functions for the Si–N, Si–Si, and N–N distances in the resulting amorphous structures.

The same plots indicate the presence of a small number of defects (the peak near 2.5 Å for the Si–Si bond, which merges with the peak that corresponds to the Si–Si distance in the second coordination sphere, and the peak near 1.6 Å for N–N bonds).

As was mentioned above, when studying charge carrier traps, we are primarily interested in defects associated with the silicon excess. These defects can be either an Si–Si bond or a single silicon atom with broken coordination (unpaired electron). In particular, the latter defect was proposed as a trap in [7]. However, the ESR signal should be observed in samples where the number of undercoordinated silicon atoms that corresponds to the concentration of traps in silicon nitride, but this signal was not observed in ESR experiments. Thus, it is reasonable to focus on the study and classification of diamagnetic Si–Si bonds as defects responsible for the memory effect in  $\text{Si}_3\text{N}_4$ .

We sought and classified Si–Si defects in the resulting structures as follows. Any pair of silicon atoms that are spaced by a distance no longer than 2.5 Å (the Si–Si distance in the second coordination sphere of the defect-free structure is  $\sim 3.1$  Å) is considered to be an

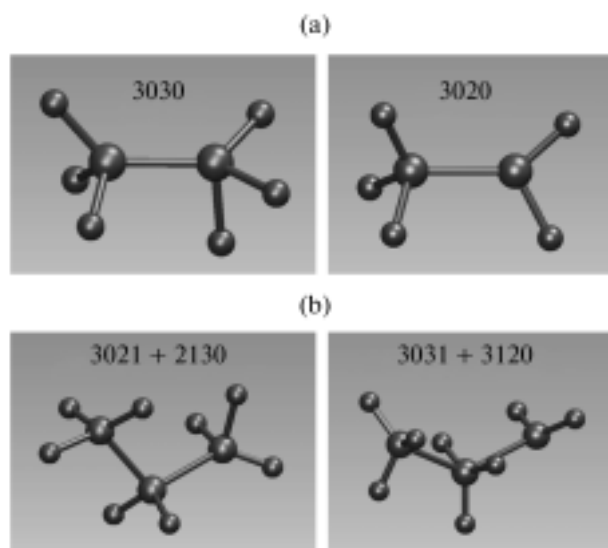


**Fig. 3.** Defects revealed in amorphous silicon nitride such as (a) Si–Si bonds and (b) double Si–Si bonds.

Si–Si bond. This threshold bond length will be justified below. For each of silicon atoms in the Si–Si bond, we sought the nearest neighbors (both silicon and nitrogen atoms) in the first coordination sphere. For the Si–N bond length, we accepted a threshold value of 2.1 Å (the Si–N bond length in the crystal is about 1.7 Å). Thus, the type of the Si–Si defect is unambiguously characterized by two silicon atoms that form the Si–Si bond and by the number of neighbors (silicon and nitrogen atoms) of each of them. It is clear that, if an additional silicon atom is located near the Si–Si bond, it is reasonable to consider such defect as a whole as a double Si–Si bond. However, to simplify the search for and notation of defects at the first stage, the double Si–Si bond (Si–Si–Si defect) was considered as two independent defects, each of which has a silicon atom, as well as a nitrogen atom, in its nearest neighboring. Correspondingly, each of the resulting Si–Si defects is denoted as  $n_{N1}n_{Si1}n_{N2}n_{Si2}$ , where  $n_{N1}$  and  $n_{N2}$  are the numbers of nitrogen atoms and  $n_{Si1}$  and  $n_{Si2}$  are the numbers of silicon atoms in the first coordination sphere of the first and second silicon atoms that form the Si–Si bond. Figure 3 shows several types of defects revealed in the resulting amorphous structure. For simplicity, we denote the 3031 + 3130 defects as 303130.

As was mentioned above, we sought defects at a threshold Si–Si bond length of 2.5 Å. This value was determined from the middle of the plateau in the pair distribution function for the Si–Si distances. When this value was increased to 2.6 Å, the number of found 4040 complexes increased sharply from 0 to about 18%. However, the 4040 complex was excluded from the consideration of the statistics of defects, because

the difference between a defect and two correctly coordinated silicon atoms that approach to 2.6 Å is very conditional in view of the strong dispersion of Si–Si distances as compared to the crystal.

The results indicate that the bond with the correct coordination (3030) is the most widespread defect (about 50% of the total number of defects) in agreement with expectations. The existence of double Si–Si bonds (the Si–Si–Si defect with different coordinations with nitrogen atoms) in a total amount of about 25% of the total number of defects that appear in the amorphous structure is an interesting and less expected result. The double Si–Si bond with the correct coordination (302130) is the most widespread modification of the Si–Si–Si bond. It is worth noting that the Si–Si–Si defect has not yet been considered as a trap for charge carriers in silicon nitride, although as was shown, this type of defects can constitute a significant part of the total number of defects in the atomic structure of amorphous silicon nitride.

Future individual investigations of each of the revealed defect types will be reasonable. In view of the results obtained above, the double Si–Si bond is of particular interest. The possibility of localization of electrons and holes should first be analyzed and the localization energy should be determined if localization is possible. The study of the revealed defects in terms of the possibility of localization of carriers

directly in the generated amorphous cell is almost senseless because of the large number of Si–Si defects (approximately ten per cell). Thus, it is necessary to find an approach that will make it possible to separate individual defects of each type in the simulated atomic structure of Si<sub>3</sub>N<sub>4</sub>.

#### REFERENCES

1. Y. Roizin, "ONO Structures and Oxynitrides in Modern Microelectronics: Material Science, Characterization and Application," in *Dielectric Films for Advanced Microelectronics* (Wiley, New York, 2007).
2. V. A. Gritsenko and S. S. Nekrashevich, *Microelectron. Eng.* **86**, 1866 (2009).
3. K. A. Nasyrov, V. A. Gritsenko, Yu. N. Novikov, et al., *J. Appl. Phys.* **96**, 4293 (2004).
4. S. Baroni, A. Dal Corso, S. de Gironcoli, et al., <http://www.pwscf.org/>.
5. P. Giannozzi, S. Baroni, N. Bonini, et al., *J. Phys.: Condens. Matter* **21**, 395502 (2009).
6. CPMD Copyright IBM Corporation. 1990–2001, Copyright MPI fur Festkoerperporschung Stuttgart 1997–2001.
7. W. L. Warren, J. Robertson, et al., *J. Appl. Phys.* **74**, 4034 (1993).

*Translated by R. Tyapaev*

SPELL: OK